Geophys. J. Int. (1990) **102,** 205–217

Stochastic inversion for scaling geology

M. Pilkington[1] and J. P. Todoeschuck[2]

[1] *Geological Survey of Canada, 1 Observatory Crescent, Ottawa, Ontario, Canada* K1A 0Y3
[2] *Defence Research Establishment Pacific, FMO, Victoria, BC, Canada* V0S 1B0

Accepted 1990 February 1. Received 1990 January 31; in original form 1989 September 26

SUMMARY

We have examined acoustic, density resistivity, gamma-ray and neutron logs from a number of boreholes in both sedimentary and igneous sequences. We show that the power spectra of these geophysical variables obey a scaling law, that is, the power spectra are proportional to some power of the frequency. In general, the power spectra are approximately inversely proportional to the frequency. This suggests that frequency-dependent noise models are more appropriate for modelling the spatial variation of geophysical parameters than the widely assumed white noise (frequency-independent) model and should be incorporated into the inversion for these variables, through *a priori* parameter covariances. The covariance of a scaling variable is simply obtained from the power spectrum. It is independent of the absolute value of the lag, that is, there is no preferred length scale, but is dependent upon the sample length.

We demonstrate the advantage of scaling noise covariances with the inversion of DC resistivity sounding data both with the exact covariance and with the approximate case of inverse proportionality. Adoption of a frequency-dependent noise model leads to a reduction in the *a posteriori* parameter variances and to solutions exhibiting a degree of smoothness commensurate with measured spatial variations of these parameters.

Key words: *a priori* constraints, inversion, scaling geology.

INTRODUCTION

The use of white noise models in the interpretation and processing of geophysical data is widespread. The assumption that members of a sequence or distribution are uncorrelated and hence exhibit a flat power spectrum has been made for mathematical simplicity and because, in many cases, little or no information about the true statistics of the population is available. For example, a random uncorrelated distribution of magnetic or gravitational sources is postulated for the spectral estimation of average source depth in the interpretation of potential field data (Spector & Grant 1970). Similarly, in the deconvolution of reflection seismic data, the assumption that the reflection coefficient sequence possesses a flat power spectrum is fundamental to the solution of this problem (Robinson 1957).

The benefits of a better statistical model are two-fold: first, it provides greater insight into the geological processes involved in rock formation and second, interpretation methods can be tailored to exploit the extra information the model provides. As an example of the latter, Todoeschuck & Jensen (1988, 1989) derived prediction error filters applicable to non-white reflection coefficient spectra and found the resulting rms error of deconvolution to be significantly reduced when the whiteness assumption was abandoned. Similarly, the correct statistical model has important consequences for generalized linear inversion methods in which the inclusion of *a priori* data in the form of parameter covariance matrices usually assumes the standard white noise model (Tarantola 1987). Even the whiteness assumption for spatial variation of parameters of interest assists in reducing the non-uniqueness of the final models and can reduce the error of fit between observed and calculated data (e.g. Parker 1988). Therefore we can expect that the use of improved parameter covariances will significantly enhance the precision and accuracy of calculated solutions.

In the following, we present evidence from borehole measurements that the use of the white noise model to describe the spatial variation of several geophysically important variables is inadequate. For the specific case of seismic measurements, we add to the growing number of observations that support a non-white reflection coefficient

sequence. Consequently, the possibility of Gaussian scaling noises (Jensen *et al.* 1990) being a more appropriate statistical model is investigated using the particular case of DC resistivity sounding inversion.

SCALING NOISES AND COVARIANCE

Scaling noises (Mandelbrot 1983, p. 351; Jensen *et al.* 1990) are stochastic series with power spectral density P, proportional to some power α, of the frequency f:

$$P \propto f^{\alpha}.$$

If the probability density function (pdf) of the series is Gaussian, we then have a Gaussian scaling noise. A Gaussian scaling noise is fully described by just three parameters: α, mean μ and the variance ε^2. Hosken (1980) proposed a scaling noise model for reflection coefficients with $0.5 \leq \alpha \leq 1.5$. He showed that this corresponds to an acoustic impedance with α of about -1. Walden & Hosken (1985, 1986) have elaborated this model and Todoeschuck, Jensen & Labonte (1990) provide additional evidence based on 21 wells from various locations in Canada with similar values of α.

The scaling noises receive that name because of the following property. If a scaling noise is originally sampled at an interval Δt and then resampled at $\Delta t'$, and the amplitude rescaled by multiplying by $(\Delta t'/\Delta t)^{-(1+\alpha)/2}$, the resultant sub-sampled sequence will appear the same as the first. The sequence is said to be self-similar after the rescaling. There is then no preferred length scale for scaling noises and they are therefore suitable for geological processes which have few typical lengths and a wide range of length scales. Self-similarity is, of course, a feature of fractals.

One of the most intriguing properties of fractals is the concept of fractal dimension. It is easy to construct fractals which are not well characterized by the normal units of length, length^2 or length^3 but can be measured in length^D, where D is not an integer. There are several more or less natural definitions of dimension for geometric fractals. It appears that natural boundaries such as coastlines have this property. The coast of Vancouver Island, for example, has $D = 1.17$. A scaling noise in x–y coordinates has $D = 2 - (1 + \alpha)/2$ for $-3 < \alpha < -1$. However, the power spectrum and the rescaling can be defined for all real α. For $\alpha = -1$, D reaches its limiting value of 2; however, cases where $\alpha > -1$ are met with in nature, most notably reflection sequences, therefore D may not be a good parameter for characterizing geology. Moreover, we will shortly consider the case where our x axis is depth but our y axis is some variable such as density. The general property of self-similarity in the broad sense is still there but there is no longer a clear notion of dimension. Cases of this sort are said to be not self-similar but self-affine (Feder 1988, p. 168). Restricting our attention to α, the slope of the power spectrum on log–log paper, keeps us out of the mathematical deep water. Indeed, the extreme sceptic can take the position that everything looks like a straight line on log–log paper without affecting the arguments we will present.

Two more properties depend upon the value of α. The first is the degree of correlation between successive values. The case $\alpha = 0$ is the familiar one of white noise. Values are completely uncorrelated and interpolation forbidden. When $\alpha > 0$, the values are anticorrelated. This is reasonable for reflection coefficients. If there is a transition from, say, a region of high velocity to a region of low velocity, it is likely that the next transition will be from low to high rather than low to lower, and the reflection coefficients will therefore have opposite signs. When $\alpha < 0$, the values are correlated to a degree depending on α. The second property is stationarity. If $\alpha > -1$ the sequence is stationary in the sense that two separated samples will have the same mean. That is we can define a mean for the process. If $\alpha < -1$ the process wanders away from its initial value and we cannot define a mean or truly define the power spectrum.

For this reason we ought strictly speaking to have referred to power spectra of samples of scaling noises. As we will always be dealing with samples this is not a serious restriction. We can calculate the expected autocovariance function from the power spectra. We will find that the autocovariance for a given lag interval depends, in a manner that is not intuitively obvious, upon the sample size and the sampling interval.

Suppose we consider a sample from a scaling noise process N points long taken at an interval Δt. Its discrete power spectrum will run from $-\omega_0 = -\pi/\Delta t$ to $\omega_0 = \pi/\Delta t$ at intervals of $\Delta\omega = 2\pi/N\,\Delta t$. The autocorrelation function is the Fourier transformation of this. The autocovariance of a non-zero mean sample is the Fourier transform of this with the $\omega = 0$ term set equal to zero, that is, with the mean removed. To examine the behaviour of the autocovariance at lag t, $\varphi(t)$, we will replace the summation by an integration. Since our model is symmetric about $\omega = 0$ we integrate over one side and multiply by 2 so that

$$\varphi(t) = \frac{P_0}{\pi} \int_{\Delta\omega}^{\omega_0} (\omega/\omega_0)^{\alpha} \cos \omega t \, d\omega,$$

$$\varphi(t) = \frac{P_0}{\pi \omega_0^{\alpha} t^{\alpha+1}} \int_{\Delta\omega t}^{\omega_0 t} (\omega t)^{\alpha} \cos \omega t \, d\omega t,$$

where P_0 is the power at ω_0. However, for the discrete autocovariance, the lag comes in units of Δt, i.e. we calculate the lag at $n\,\Delta t$. Then

$$\varphi(n\,\Delta t) = \frac{P_0 \omega_0}{\pi^{\alpha+2} n^{\alpha+1}} \int_{2\pi n/N}^{n\pi} u^{\alpha} \cos u \, du.$$

Let us examine the behaviour of the integral

$$I = \int_a^b u^{\alpha} \cos u \, du$$

as the lower limit a approaches zero from above. For $\alpha > 0$ the integrand obviously remains finite and I is well behaved in the limit $\alpha \to 0$. We may integrate I by parts:

$$I = \frac{u^{\alpha+1} \cos u}{\alpha + 1} \Bigg|_a^b + \int_a^b \frac{u^{\alpha+1}}{\alpha + 1} \sin u \, du.$$

For $0 > \alpha > -1$ the first term and the integrand of the second term remain finite as $\alpha \to 0$, but for $\alpha < -1$, I diverges as $N \to \infty$. This means that the value of the autocovariance depends on the sample length for $\alpha < -1$. For $\alpha > -1$ we can assume N is large and replace the lower

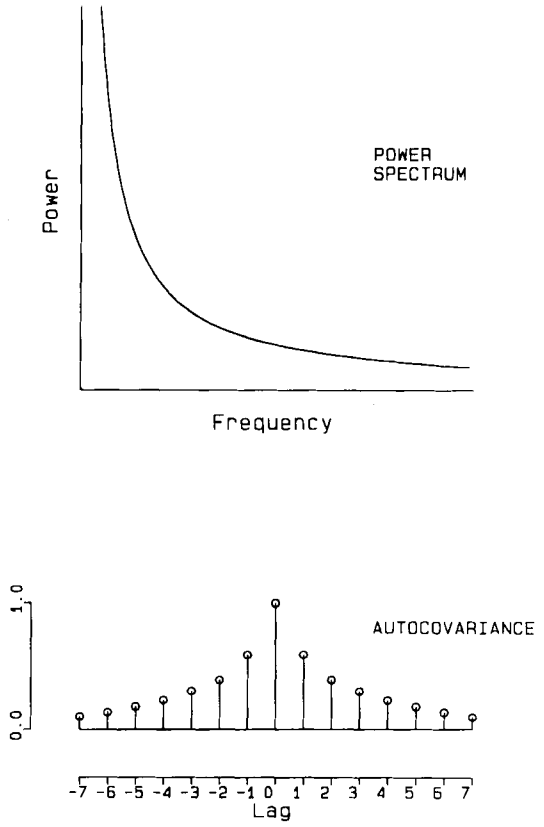

Figure 1. Power spectrum and autocovariance functions for $\alpha = -1$.

limit by zero. Then the lag term $\varphi_0 = \varphi(0)$ is given by

$$\varphi_0 = \frac{P_0 \omega_0}{\pi(\alpha + 1)},$$

while in general

$$\varphi(n\,\Delta t) = \varphi_n = \frac{P_0\omega_0}{\pi(\alpha+1)}\left(\frac{\alpha+1}{\pi^{\alpha+1}n^{\alpha+1}}\int_0^{n\pi} u^\alpha \cos u\,du\right)$$
$$= \varphi_0\left(\frac{\alpha+1}{\pi^{\alpha+1}n^{\alpha+1}}\int_0^{n\pi} u^\alpha \cos u\,du\right).$$

This means that the autocovariance normalized by dividing by φ_0 is independent of the absolute or physical lag, depending for a given α only on n. No concept such as correlation length can be defined. This is perhaps the clearest indication of scaling characteristics.

In any event, it is very easy to determine the expected autocovariance for a given model sample size and interval by calculating the discrete inverse Fourier transform of the appropriate power spectrum. Fig. 1 shows a typical case.

BOREHOLE DATA

Before examining the actual data it is worth asking if there is any argument for α having a particular value for variables such as resistivity or density. Geology is clearly correlated, therefore we might expect $\alpha < 0$. Furthermore, if we neglect gravity and compressibility we can conceive of an infinite formation of rock types which would vary from place to place but never to some drastically different substance. Density for example would never approach infinity. Alternatively, we may view the local geology as a sample of a very long time sequence of rock types at any one point. In other words we might imagine that geology is stationary in the mean in the sense described above. The most correlation with stationarity is for $\alpha = -1$. This argument was applied in Todoeschuck & Jensen (1988) to acoustic impedances and there is no reason against it for other variables.

Measurements presented below are from the borehole geophysics test area at Bells Corners, Ottawa, Canada. The six holes are spaced up to 100 m apart with the three longer holes reaching a depth of 300 m and the three shorter, approximately 150 m. In this area, the top 65 m of Upper Cambrian and Ordovician sandstones and dolomites of the Nepean Formation are separated from the underlying Precambrian granite and gneisses of the Grenville Complex by a thick weathered alteration zone. Several fracture zones exist through the section (Bernius 1981). For the spectral calculations, the data from each hole were partitioned into sedimentary and igneous sections and the weathered zone avoided. Fig. 2 shows a representative log taken from well BH5 where the sampling interval for all parameters is 0.1 m.

Power spectra were estimated using the periodogram method. For each original digital log, the average was removed, the data tapered to zero with a taper length of 25 samples and padded with zeros such that the final data length was equal to a power of 2. A total of 512 values were used for the sedimentary section and up to 2048 for the igneous. After Fourier transformation, the raw periodograms were then smoothed by three passes of a standard three-point smoothing filter (coefficients: $\frac{1}{4}$, $\frac{1}{2}$, $\frac{1}{4}$). Fig. 3 shows representative log–log power spectral plots for the various parameters taken from well BH5 and Table 1 shows the results of least-squares line fitting to the spectra.

Power spectra for acoustic impedance were calculated using velocity and density information, and velocity data alone. Walden & Hosken (1985) have found scaling noise behaviour in reflection coefficient spectra calculated from velocity data alone for seven out of eight logs studied. The effects of including density data in the computation of acoustic impedance were found to be minimal and do not effect the observed scaling behaviour. Values of α range from 0.55 to 1.5 (both in igneous rocks) with averages of 0.86 for sediments and 0.92 for igneous rocks. Since the results are based on such a small sample, this difference is not expected to be significant. The above values for sedimentary rocks fall within the range of Walden & Hosken (1985) and are close to those of Todoeschuck *et al.* (1990).

Importantly, igneous rocks sampled also show scaling behaviour over these length scales (1–100 m). This suggests the use of scaling-type prediction error filters (Todoeschuck & Jensen 1988, 1989) for the deconvolution of deep reflection seismic data such as that collected for regional lithospheric studies e.g. COCRUST, Lithoprobe. Although igneous structure is more closely 3-D than sedimentary, we can expect a significant improvement using the scaling hypothesis. Additionally, well-log data extend the range of scaling behaviour which has been observed over length scales of 20 m to 1 km as evinced from seismic wave scattering (Wu & Aki 1985).

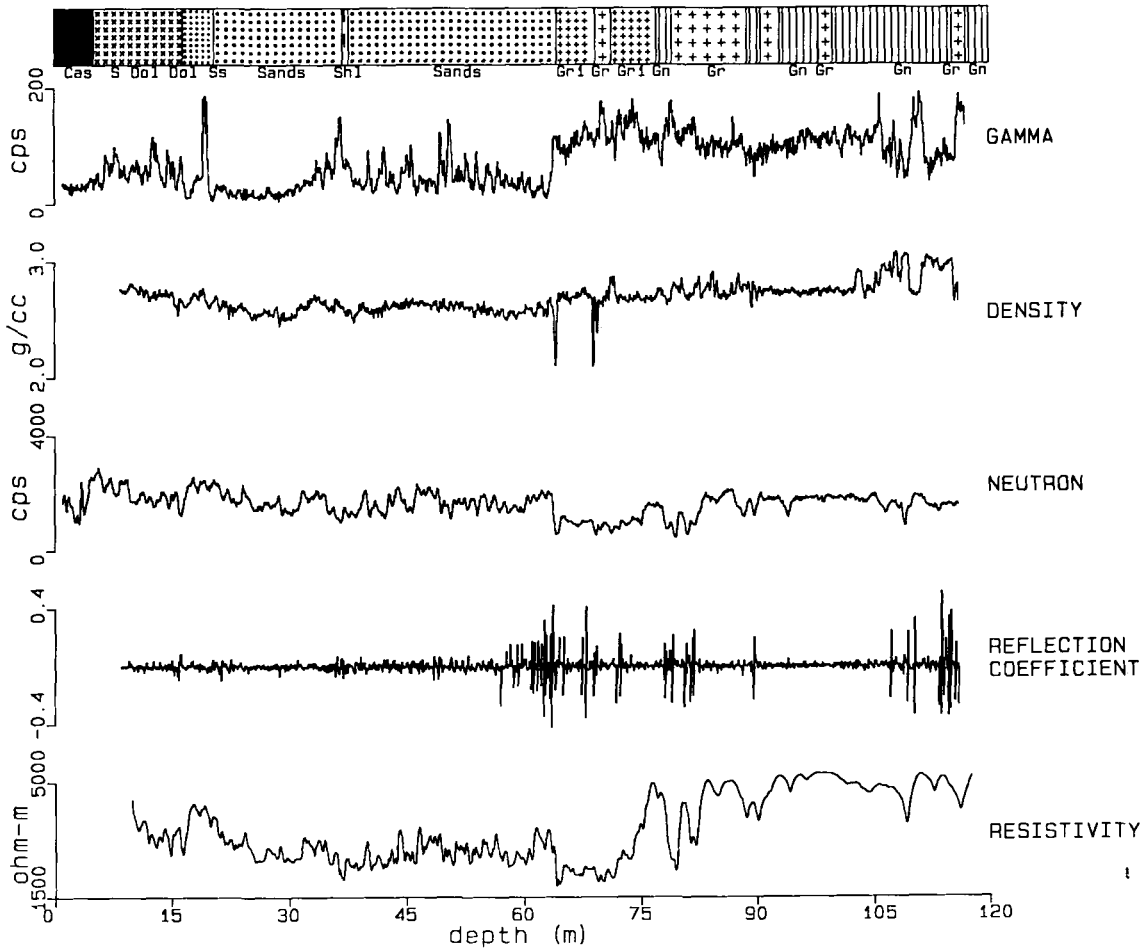

Figure 2. Representative log (BH5) from the Bells Corners area. The weathered zone between the sedimentary and igneous sections (60–65 m) is clearly outlined on all logs. Note the resistivity measurement scale is logarithmic.

Resistivity data were obtained using a standard short normal configuration in which the current and measurement electrodes are placed 0.4 m apart. In a homogeneous isotropic medium, 50 per cent of the potential drop towards zero occurs within a sphere of radius equal to the measurement-current electrode spacing. Equating this distance with the resolving limit of the logging tool, the vertical resolution limit of the data possible is then 0.8 m. Even though the spectra are plotted up to the Nyquist frequency (5 cycles m^{-1} for a sampling interval of 0.1 m), only that part of the spectrum below the resolving limit of the logging tool is used for the estimation of the scaling exponent. This limit is indicated by a dashed line in Fig. 3. Power spectra of resistivity logs show average values of the scaling exponent, $\alpha = -1.0$ for the sediments and -1.4 for the igneous section.

Density data were collected with a single detector gamma–gamma logging tool. The depth of investigation of the tool increases with decreasing formation density but usually does not exceed 0.15 m. Therefore the vertical resolution possible is limited by the detector–source separation of 0.4 m. Fig. 3 shows an average $\alpha = -1.2$ for sediments and $\alpha = -1.1$ for igneous rocks. All of the density logs show spectra indicative of more than one slope, i.e. multiscaling behaviour. Specifically, the logs show relative increases in power at low frequencies. This suggests that (at least) two different geological/physical processes were active, each with a characteristic bandwidth and value of α. Wu & Aki (1985) observed similar behaviour with respect to lithospheric inhomogeneities detected by seismic wave scattering. In the case of density variations, it is probable that an increase in low-frequency power results from compaction effects superimposed on an apparent linear fall off in power at higher frequencies.

Natural gamma radiation was recorded with a NaI crystal scintillation counter which measures the total contribution (total count) due to the presence or uranium, thorium and potassium. The total count in sediments is usually indicative of shale content while in igneous rocks, it correlates with the level of K-feldspar. The tool only responds to a small area around the detector due to the attenuating effects of the medium, which increase with density and a decrease in the gamma radiation energy level. In a homogeneous medium, the contribution of the sphere centred on the detector falls to 50 per cent at a radius of 0.2 m. Hence, the vertical resolution of the tool can be taken as 0.4 m. The power spectra of the gamma-ray logs give an average of $\alpha = -0.72$ for the sediments and -0.91 for igneous rocks.

Neutron logs were measured with a sidewall neutron porosity tool which senses the epithermal neutron density of

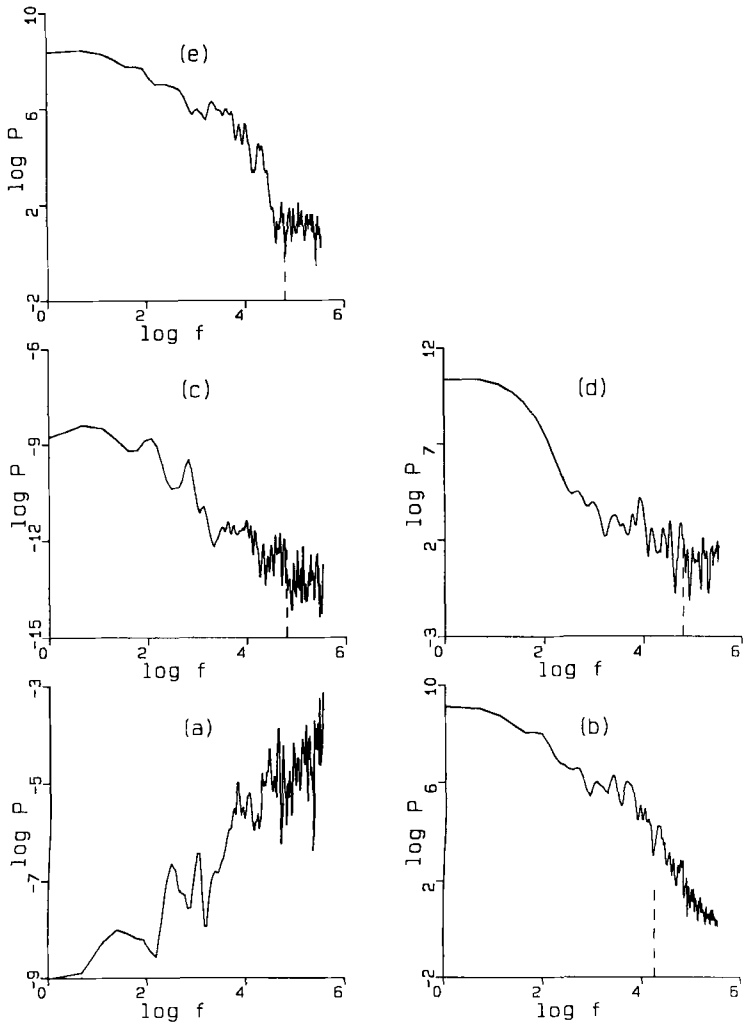

Figure 3. Power spectra of (a) reflection coefficients (b) resistivity data (c) density data (d) natural gamma radiation and (e) neutron density for the sedimentary section of the Bells Corners log BH5. Dashed vertical lines indicate the resolving limit of each logging tool.

the formations. Neutron logs measure the apparent concentration of hydrogen atoms per unit volume (hydrogen index), which is a direct measure of porosity. As with the resistivity and gamma-ray log, there exists a sphere of influence throughout which the log responds to. This decreases with increasing porosity and if the limit is defined as that radius at which 90 per cent of the total measurement responds to, this is equal to 0.35 m for 10 per cent porosity. Generally, the vertical resolution is slightly larger than the source–detector spacing, which for the sidewall neutron log is 0.4 m. Neutron log spectra show average scaling exponents of -0.99 for the sedimentary section and -1.2 for the igneous.

Thus, power spectra of several important geophysical variables show scaling noise behaviour over at least some range of spatial frequencies in the logs we have examined and in particular favour $\alpha = -1$. The implications of the non-zero α are clearly far-reaching, in particular the extra information and stabilizing effects of α when utilized as *a priori* data in the inversion of geophysical data.

Fitting a single straight line to the spectra is probably an oversimplification of the whole geological problem. There is a definite temptation to fit the spectra with more complicated functions [a 'multifractal' approach: Feder (1988, p. 66)] or at least with several line segments [corner frequencies: Walden & Hosken (1985), for the reflection sequence, and an anonymous reviewer for the rest]. We resist the temptation. All we have are estimates of the power spectrum and rather noisy ones at that. In particular, the low frequencies, exaggerated in importance by a log–log plot, are only represented in our data by a few cycles. Furthermore, we are looking for the minimum number of extra *a priori* assumptions for the inversion problem. One extra parameter seems about right but other models are certainly possible. A fit to a white spectrum below a corner frequency prevents the divergence of the autocovariance with sample length but we would still have to take into account the sample interval. Of necessity, we are concerned with finite examples and, as explained above, when we calculate our expected model covariances, the question of divergence does not arise.

There are many other interesting questions to be asked. Are the probability distribution functions adequately described as Gaussian? In the case of reflection sequences for a different data set, Todoeschuck *et al.* (1990) showed that this was bound up intimately with the question of

Table 1. Scaling exponents (α) and associated correlation coefficients (R) resulting from least-squares line fitting to the observed spectra for wells BH1–6 at Bells Corners. Spectral estimates above the resolution limit indicated in Fig. 3 were excluded from the line fitting.

RESISTIVITY

	Sedimentary		Igneous	
	α	R	α	R
BH1	-1.1±.06	-.93	-1.5±.09	-.92
BH2	-.96±.08	-.86	-1.8±.08	-.95
BH3	-1.2±.07	-.93	-1.9±.10	-.93
BH4	-1.0±.07	-.92	-1.0±.08	-.87
BH5	-1.1±.08	-.91	-1.2±.11	-.86
BH6	-.80±.06	-.88	-1.3±.08	-.92

DENSITY

	Sedimentary		Igneous	
	α	R	α	R
BH1	-1.4±.08	-.93	-1.1±.06	-.92
BH2	-1.3±.09	-.90	-1.7±.06	-.97
BH3	-1.3±.10	-.89	-1.1±.06	-.93
BH4	-.87±.09	-.82	-.71±.07	-.83
BH5	-1.2±.09	-.93	-.91±.06	-.90
BH6	-1.2±.08	-.90	-1.1±.07	-.82

REFLECTION COEFFICIENT

	Sedimentary		Igneous	
	α	R	α	R
BH1	.73±.07	0.83	.55±.07	0.76
BH2	.84±.09	0.80	.87±.05	0.91
BH3	.66±.07	0.78	.77±.10	0.76
BH4	1.0±.08	0.88	1.5±.09	0.94
BH5	1.1±.09	0.88	1.3±.07	0.92
BH6	.84±.05	0.92	1.3±.08	0.92

NEUTRON

	Sedimentary		Igneous	
	α	R	α	R
BH1	-1.1±.05	-.94	-1.2±.08	-.91
BH2	-.93±.06	-.92	-1.4±.08	-.94
BH3	-.98±.05	-.93	-1.5±.08	-.93
BH4	--------	-----	--------	-----
BH5	-.97±.07	-.89	-.94±.10	-.80
BH6	-.97±.08	-.87	-.91±.05	-.94

GAMMA

	Sedimentary		Igneous	
	α	R	α	R
BH1	-----	-----	-----	-----
BH2	-----	-----	-----	-----
BH3	-.42±.03	-.87	-.98±.10	-.81
BH4	-.76±.05	-.91	-.69±.06	-.85
BH5	-.90±.10	-.81	-1.1±.08	-.89
BH6	-.81±.13	-.94	-.88±.06	-.79

stationarity. The geological interpretation of the spectra is unclear. Should we regard ourselves as sampling from 'Geology' as a whole, from geology of a certain type, or of a geological province? How are lithologies represented or the divisions drawn by geologists on a section? Fortunately, we do not have to answer these questions to deal with the problem at hand. Our only interest is in the power spectra and what they imply for the covariances.

INVERSION AND *A PRIORI* DATA

The inversion of any geophysical data requires the undertaking of two interrelated problems: solution construction and solution appraisal. The former involves the determination of a set of model parameters which, based on known theory, predict the observed data to within a prescribed degree of accuracy. No matter how sophisticated the methodology for finding an acceptable solution, nor how much information concerning our prior knowledge of the problem at hand is incorporated into the inversion, the single model thus determined only represents the first step to a more complete answer to the problem. In order to achieve a fuller understanding of the solution e.g. through estimates of its precision and accuracy, we must also address the problem of solution appraisal.

A priori data, whether in the form of statistics of parameters and data or parameter bounds imposed by physical arguments plays a pivotal role in both the construction and appraisal of the solution to a given inverse problem. A large number of inverse problems are ill-posed in that small changes in the model parameters may cause correspondingly large variations in the predicted data. Constructing a suitable inverse operator to recover parameter estimates from observed data requires some form of stabilization or regularization (Tikhonov 1963). For non-linear problems, the regularization or damping of successive parameter corrections in an iterative search for a solution ensures that the linear approximations adopted still hold and unwanted oscillatory effects in the model are kept to a minimum. This is an *ad hoc* approach and therefore permits flexibility in choosing the appropriate amount of damping for a particular problem. Generally, as the severity of regularization increases, convergence of the iterative search decelerates and the final model becomes smoother (possibly at the expense of a poorer fit to the data). The commonest approaches to damping either involve adding a constant to the problem eigenvalues (Marquardt 1963) or removing the effects of near-zero and zero eigenvalues from the solution (Wiggins 1972). The use of regularization in solution construction can be regarded merely as a computational convenience to ensure the existence of one solution to the problem, although damping has a probabilistic interpretation which will be discussed below.

Returning to the second part of the inverse problem, the appraisal of a given solution, regularization provides a means of incorporating all available prior information about the problem. This has the effect of reducing the degree of non-uniqueness of the final model estimates. Additionally, the extra information content of the prior data can be expected to reduce the final parameter errors and provide a more complete and realistic description of their behaviour as measured by the *a posteriori* covariances than that provided by the data alone. Two methods of incorporating prior information which differ in their philosophical approach but may lead to similar computational methods are Bayesian inference (Backus 1970; Tarantola & Valette 1982) and stochastic inversion (Franklin 1970; Jackson 1979).

Bayesian inference (BI) has found geophysical applications ranging from computation of regional stress tensors (Angelier *et al.* 1982) to determining magnetic fields at the Earth's core (Gubbins & Bloxham 1985). Based on Bayes'

rule, BI quantifies the modification of the *a priori* of the parameters by information provided by the measurements resulting in an *a posteriori* pdf which constitutes the solution to the inverse problem (Duijndam 1988). The *a priori* information can be derived from physical arguments e.g. non-negative densities or propagation velocities, which lead to linear or quadratic constraints on the parameters. These bounds are 'hard' (Jackson 1979) because the pdf of the parameters outside the bounds is zero. Softer bounds can also be used; these usually take the form of a pdf such that the same physical reasoning can be used but there is now a non-zero probability that the parameters may take on some value outside the original bounds. BI has the advantage of allowing subjective priori beliefs to be included in the inversion, that is, personal choices can be made in constructing the *a priori* parameter pdf (Backus 1988). Note that the non-trivial decision of how the model is parametrized (e.g. thickness of layers) is equivalent to imposing a prior belief on the behaviour of the final model character.

Stochastic inversion (SI), on the other hand, is a more objective approach to inverse problems and provides the same results independent of the interpreters prior knowledge. As formulated by Franklin (1970), the model parameters are assumed to be the realization of a second-order Gaussian process whose mean and variance are known. The stochastic inverse then minimizes the variance of the parameter estimation errors and represents a rational way of estimating a random vector of parameters from measurements whose error statistics are known. Jackson (1979) showed that the Gaussian assumption is not necessary and that the stochastic inverse is insensitive to the pdf of the parameters. Obviously, if covariance information for the model is available from some independent source, such as a previous inversion in a similar geological environment or from direct measurements of some physical property e.g. through well-logging, SI provides the most natural method of inverting the data. It will result in an objective level of regularization used in the construction of a solution in that the model is not smoothed to some arbitrary degree but has properties in keeping with previous measurements. Similarly, the important questions of how the model estimate is determined by the combination of prior data and observations and what the relative contribution of the two is can be addressed in a meaningful way.

In the following, we use stochastic inversion with a particular type of *a priori* parameter covariance based on direct measurements of rock properties from borehole measurements: the scaling noise model. Importantly, we show that this class of covariance function has important consequences for both the existence and uniqueness of the computed solutions. Additionally, we find that using this type of information, the final model naturally exhibits the appealing property of smoothness.

STOCHASTIC INVERSION

For the general non-linear inverse problem, the relation between model parameters and data can be written

$$\mathbf{y} = f(\mathbf{x}) + \mathbf{e} \tag{1}$$

where $\mathbf{y}$ is an n-vector of data values, $\mathbf{x}$ is an m-vector of model parameters, $\mathbf{e}$ is an n-vector of data errors and $f()$ is a non-linear functional through which the effects of model $\mathbf{x}$ can be calculated. The solution to equation (1) is achieved by the minimization of the misfit between observed and calculated data and some norm of the model, i.e.

$$\min_{\mathbf{x}} [\mathbf{y} - f(\mathbf{x})]^{\mathrm{T}} \mathbf{D}^{-1} [\mathbf{y} - f(\mathbf{x})] + (\mathbf{x} - \mathbf{x}_0)^{\mathrm{T}} \mathbf{P}^{-1} (\mathbf{x} - \mathbf{x}_0) \tag{2}$$

where $\mathbf{x}_0$ is the *a priori* estimate of the model parameters which have covariance $\mathbf{P}$ and $\mathbf{D}$ is the data error covariance matrix. In equation (2) the second term minimizes the quadratic norm with respect to the *a priori* model. The effects of $\mathbf{D}$ and $\mathbf{P}$ reduce the influence of data and parameters that have large variances and also scale parameters to a dimensionless form. The solution of equation (2) leads to the iterative algorithm (Tarantola & Valette 1982)

$$\mathbf{x}_{k+1} = \mathbf{x}_0 + \mathbf{P}\mathbf{A}_k^{\mathrm{T}} (\mathbf{A}_k \mathbf{P} \mathbf{A}_k^{\mathrm{T}} + \mathbf{D})^{-1} [\mathbf{y} - f(\mathbf{x}_k) + \mathbf{A}_k (\mathbf{x}_k - \mathbf{x}_0)] \tag{3}$$

where $\mathbf{x}_k$ is the current model estimate at iteration k and

$$\mathbf{A}_k = \left. \frac{\partial f}{\partial \mathbf{x}} \right|_{\mathbf{x} = \mathbf{x}_k}. \tag{4}$$

An equivalent form of equation (3) can be derived for overconstrained systems (Tarantola & Valette 1982); however, we will only consider the underdetermined problem, i.e. $n \ll m$. This is a more appropriate form since in theory we are attempting to model a continuous function from a finite set of data. Also, by effectively overparametrizing the problem, the role played by the *a priori* information is not obscured by the effects of the particular model parameterization chosen. The *a posteriori* covariance of the parameters determined from equation (3) is given by

$$\mathbf{C} = \mathbf{P} - \mathbf{P}\mathbf{A}_\infty^{\mathrm{T}} (\mathbf{A}_\infty \mathbf{P} \mathbf{A}_\infty^{\mathrm{T}} + \mathbf{D})^{-1} \mathbf{A}_\infty \mathbf{P} \tag{5}$$

where $\mathbf{A}_\infty$ contains the partial derivatives of the data with respect to the parameters evaluated at the acceptable final solution. Equation (5) is only strictly true for linear problems, but if the non-linearity is not strong in the vicinity of the final model then $\mathbf{C}$ can be found approximately in this fashion.

If $\mathbf{P}$ and $\mathbf{D}$ have neither null variances nor perfect correlations they will both be positive definite and the inverse in equation (5) will exist. Hence, the *a posteriori* variances will be smaller or equal to the priori variances. By examining the reduction in the variance of individual parameters, the amount of information provided by the measurements can be assessed and the relative contribution of *a priori* and observational data to the final parameter values found.

Two extreme situations occur concerning the covariance $\mathbf{C}$. When the data do not contribute to the solution of the problem, $\mathbf{C} = \mathbf{P}$, and there is no reduction in the parameter variances. If the *a priori* covariances are infinite, then $\mathbf{C} = (\mathbf{A}^{\mathrm{T}} \mathbf{D} \mathbf{A})^{-1}$ and the variance of the model is merely the result of propagation of data uncertainty into the solution. A tool similar to covariance analysis used in solution appraisal is the resolution matrix $\mathbf{R}$ defined by

$$\mathbf{x}_\infty - \mathbf{x}_0 = \mathbf{R}(\mathbf{x}_t - \mathbf{x}_0) \tag{6}$$

where $\mathbf{x}_\infty$ is an acceptable solution and $\mathbf{x}_t$ is the true model

we are seeking. Using equations (1) and (3) we find

$$\mathbf{R} = \mathbf{P}\mathbf{A}_\infty^{\mathrm{T}}(\mathbf{A}_\infty\mathbf{P}\mathbf{A}_\infty^{\mathrm{T}} + \mathbf{D})^{-1}\mathbf{A}_\infty. \quad (7)$$

Backus & Gilbert (1970) showed that the correction to the *a priori* model in equation (6) is a filtered or averaged version of the true correction, with the rows of **R** (resolving kernels or averaging functions) quantifying the type of averaging. If **R** is close to the identity matrix then $\mathbf{x}_\infty$ approaches the true solution, otherwise we must be satisfied with some (smoother) linear combination of the true model parameters. From equations (5) and (7) the *a posteriori* parameter covariance can be written (Tarantola 1987, p. 494)

$$\mathbf{C} = (\mathbf{I} - \mathbf{R})\mathbf{P}. \quad (8)$$

It is clear that as $\mathbf{R} \rightarrow \mathbf{0}$, the parameters are poorly determined by the data and $\mathbf{C} \rightarrow \mathbf{P}$, resulting in no reduction of the model variance by the measurements. However, if $\mathbf{R} = \mathbf{I}$ (parameters perfectly resolved by the data), then $\mathbf{C} \rightarrow \mathbf{0}$ only if $\mathbf{D} \rightarrow \mathbf{0}$, otherwise the standard least-squares estimate of covariance should be used (Nowack & Lutter 1988). Equation (8) illustrates the trade-off between resolution and variance of the model parameters. As **P** increases (our prior information becomes poorer), more weight is placed on the data misfit term in equation (2) and the resolution improves at the expense of greater variance in the final solution as measured by **C**. Obviously, from the above discussion, the measures used in appraising the solution are only meaningful to the degree of how realistic our **P** is.

Estimated data errors have long been incorporated into the inversion of geophysical data, however, only recently has any attempt been made to exploit the extra information provided by *a priori* parameter covariances. Most studies have then only used uncorrelated covariance functions, resulting in a diagonal **P** (van de Meulebrouck, Bayer & Burg 1984; Gubbins & Bloxham 1985; Bloxham 1987). Jackson (1979) argues that for problems with a small number of parameters the off-diagonal elements in **P** can be neglected as long as the diagonal terms are increased in compensation. However, when dealing with an overparametrized problem, the significance of the off-diagonal elements increases.

Constable, Parker & Constable (1987) and Meyerholtz, Pavlis & Szpakowski (1989) introduced off-diagonal terms in **P** with a view to deriving smooth solutions. The rows of **P** are specified to be finite difference approximations to first or second derivative operators so that the quadratic norm $\mathbf{x}^{\mathrm{T}}\mathbf{P}^{-1}\mathbf{x}$ becomes a measure of model roughness which is minimized in a similar fashion to equation (2). The incorporation of smoothness constraints on final models has recently found increasing use in addressing the problem of non-uniqueness in the inversion of geophysical data (Parker & Shure 1982; Constable *et al.* 1987; Meyerholtz *et al.* 1989). Originally suggested by Backus (1970) as a method for ensuring that the linear functionals making up **A** were members of a Hilbert space, smoothing or quelling is particularly necessary when constraints on the model imposed by the chosen parametrization are weak e.g. the sub-surface is divided into a large number of layers whose individual thickness is smaller than that resolvable by the data. Then, rather than investigating the non-uniqueness by computing a number of models which all fit the data and finding features in common (which are likely to be shared by the true model), the smoothest model permissible by the data is calculated. This solution has the maximum simplicity demanded by the data and is less likely to be corrupted by small-scale variations of which we are unsure whether they exist in the true model. Additionally we can be confident that the true model must be at least as, but never less complex than this smooth solution (Constable *et al.* 1987).

Using the philosophy of Bayesian inference, Tarantola & Valette (1982), Tarantola & Nercessian (1984) and Montagner & Jobert (1988) have used *a priori* covariance functions of a Gaussian form:

$$P(x_1, x_2) = \sigma^2 \exp\left[-(x_1 - x_2)^2\right]/L^2 \quad (9)$$

which implies a variance of σ^2 at position x_1 and a correlation between parameters x_1 and x_2 dependent on the length L. Since L acts as a trade-off parameter in the sense of Backus & Gilbert (1970), Montagner & Jobert (1988) increase L until the improvement in resolution is accompanied by a much larger increase in parameter variance. This L is then used in the final inversion. So, although the inclusion of off-diagonal terms in **P** is more realistic, the *a priori* information is arbitrarily varied to suit the needs of the interpreter. This is not acceptable within the framework of stochastic inversion where there should only be one correct measure of the *a priori* covariance (the same for all interpreters)—that based on samplings of the distribution in which the true model lies.

Using the scaling noise covariance functions discussed earlier, the process variance ε^2 takes on the role of a trade-off parameter. The *a priori* parameter covariance matrix can be written explicitly in terms of α and ε^2,

$$\mathbf{P} = \varepsilon^2\mathbf{E}^*\mathbf{F}\mathbf{E}, \quad (10)$$

where **E** and **E*** are the matrix equivalents of Fourier and inverse Fourier transformation (Kanasewich 1981) and **F** is a diagonal matrix whose ith element is f_i^{α}, where f is frequency. Equation (10) decomposes **P** into eigenvalues and eigenvectors. Thus, decreasing ε increases the eigenvalues of $\mathbf{P}^{-1}$ and more weight is placed on the quadratic term in equation (2). From equation (7), parameter resolution is then degraded but the parameter variances in equation (8) are also decreased. When using **P** of the form in equation (10) with $\alpha < 0$, the quadratic norm $\mathbf{x}^{\mathrm{T}}\mathbf{P}^{-1}\mathbf{x}$ gives a measure of solution roughness, since for $\alpha = -1$, equation (2) is equivalent to minimizing the first derivative of the parameter vector **x**. For $\alpha = -2$, equation (2) minimizes the second derivative of **x**, and so on. For variables such as resistivity, density and acoustic impedance (Table 1), well-log measurements show that $\alpha < 0$, so the norm in equation (2) imposes a smoothness constraint on the solution. However, for reflection coefficients, which show $\alpha > 0$, the solution is constrained to be rough, in keeping with observed characteristics of these types of sequences.

Importantly, knowledge of α determines the correct amount of smoothing to be used in inversion, rather than specifying some *ad hoc* or favourite level. Consequently, the solution may be smoother or rougher than we would normally deem fit. However, no subjective constraints have

been imposed on the model and the calculated solution is only that supported by the observational and *a priori* data.

RESULTS

In this section, an example of the use of scaling noise covariance functions is illustrated for the case of DC resistivity sounding data. The data consist of borehole resistivity measurements from well BH3 of the Bells Corners logging test site discussed earlier. For inversion purposes, the original log was resampled at a 1 m interval and apparent resistivities calculated for a simulated Schlumberger spread starting at $AB/2 = 1$ m with eight samples per decade using the algorithm of Koefed (1979). A total of 25 data was generated from the 100 layer model (Fig. 4). The model is terminated below by a half-space of resistivity equal to the logged resistivity at a depth of 100 m. In the following examples, the models are parametrized as $\log_{10}$ (layer resistivity) with the layer thickness held constant throughout the inversion.

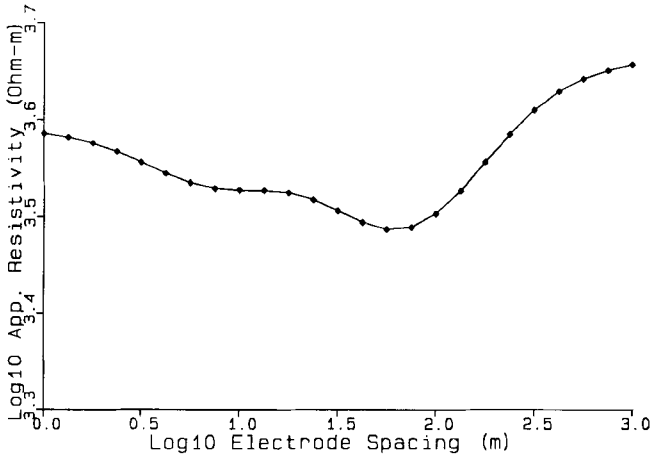

Figure 4. Sounding data generated from well BH3 assuming 100 layers of thickness 1 m for a Schlumberger spread starting at an electrode spacing ($AB/2$) of 1 m.

The scaling exponent α was determined from a least-squares straight line fit to the power spectrum of the resistivity log. Fig. 5 shows the spectrum and the best fitting line with $\alpha = -1.5$. Using this value of α, **P** was constructed in the manner of equation (10). For comparative purposes, inversions with $\alpha = 0$ (white noise covariance function) and $\alpha = -1.5$ (scaling noise) were carried out. The same value of the process variance ($\varepsilon^2 = 28\,600\ \Omega^2\text{m}^2$) was used for each inversion. Fig. 6 shows the results of inverting the data of Fig. 4 using the algorithm of equation (3) along with the true (logged) resistivities. The borehole data exhibits small-scale structure beyond the resolving power of the simulated sounding data; however, we can expect to recover the gross features of the true resistivity distribution. Fig. 5 shows that with the white noise assumption, inversion recovers the true structure well down to 20 m but deeper the match is relatively poor even though the calculated resistivities exhibit some fine-scale features such as the resistivity low at 38–50 m depth.

In comparison, the scaling noise inversion ($\alpha = -1.5$) recovers the main features of the true resistivity well but is much smoother than the $\alpha = 0$ model. Both inversions resulted in similar levels of data misfit but the scaling model represents that model with a degree of smoothness in keeping with the correlation lengths determined from the borehole data. For this reason, and because the rougher white noise model may contain features that are not required by the data, the scaling inversion results are to be preferred.

In addition to solution smoothness, the scaling noise model provides more useful information in terms of the accuracy and reliability of the solution than the white noise model. Fig. 7 shows resolving kernels for parameters equal

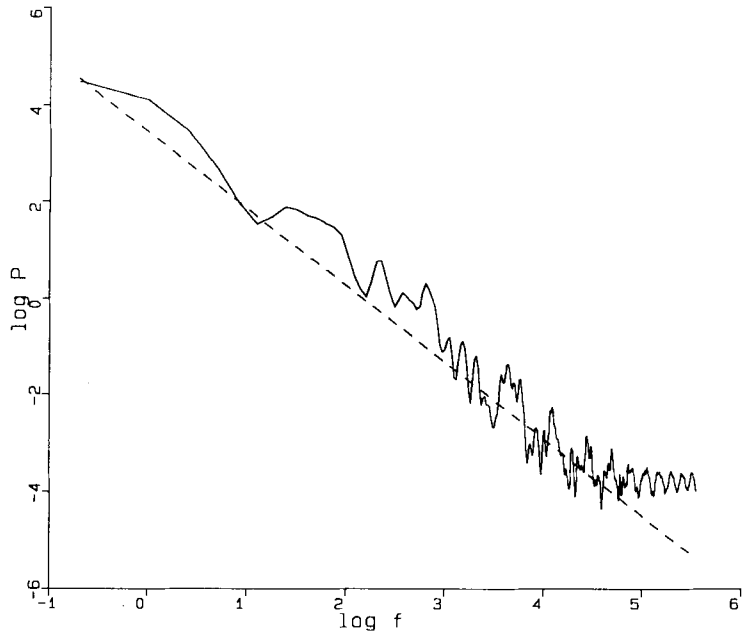

Figure 5. Power spectrum of the BH3 resistivity log and the best fitting straight line in a least-squares sense. Line slope is (α) −1.5. This value of α is used to construct the *a priori* parameter covariance matrix for inversion.

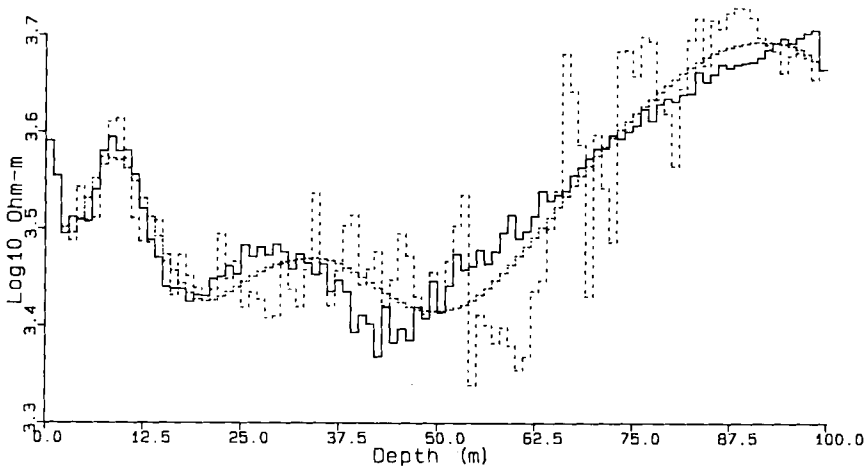

Figure 6. Inversion results for the BH3 simulated sounding: longer dashed line represents the true (logged) resistivities, solid line is f^0 inversion (white noise covariance model), dotted line is $f^{-1.5}$ inversion (scaling noise covariance model). Note that the f^0 inversion does not match the true resistivities well. The scaling noise model produces a smooth fit to the logged resistivities. The starting model for all inversions is a half-space of resistivity 3000 Ω m.

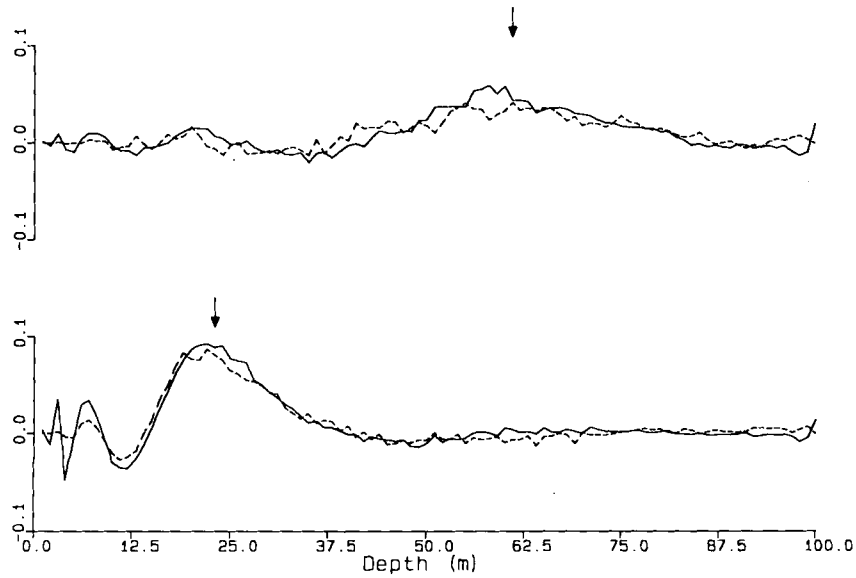

Figure 7. Resolving kernels (rows of the resolution matrix **R**) for layers at 23 (upper part of figure) and 61 m depth. Arrows indicate the positions of the layers. Dashed line is f^0 inversion, solid line is $f^{-1.5}$.

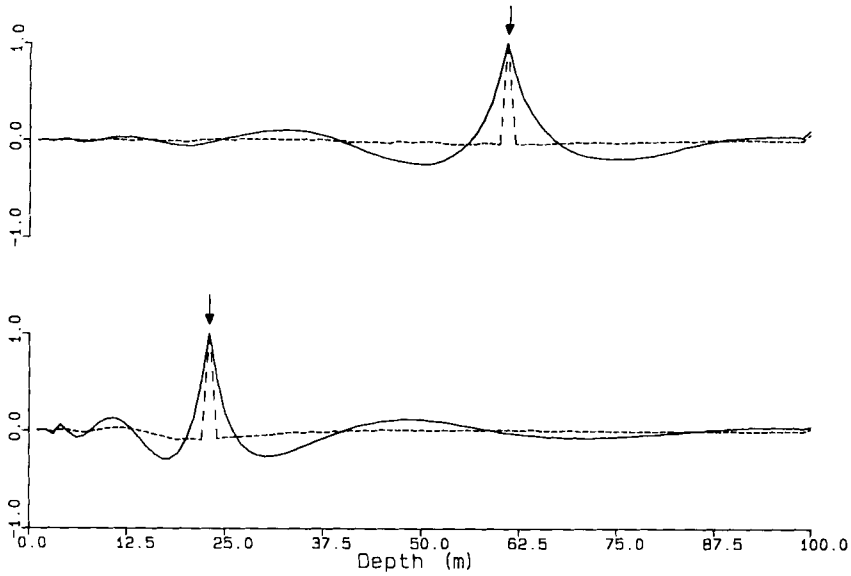

Figure 8. Correlation functions (rows of the *a posteriori* parameter covariance matrix standardized to have unit variance) for layers at 23 (upper part of figure) and 61 m depth. Arrows indicate the positions of the layers. Dashed line is f^0 inversion, solid line is $f^{-1.5}$.

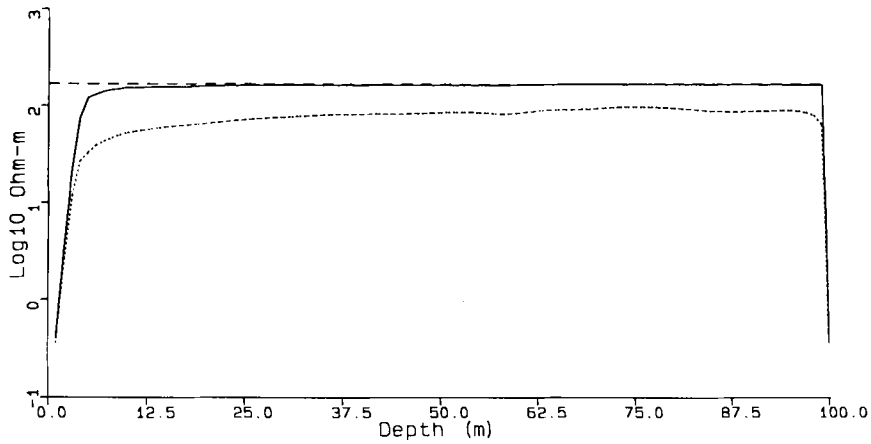

Figure 9. Standard deviations of layer resistivities: horizontal dashed line is the *a priori* parameter standard deviation (169 Ω m), solid line $\alpha = 0$ inversion and dashed line $\alpha = -1.5$ inversion.

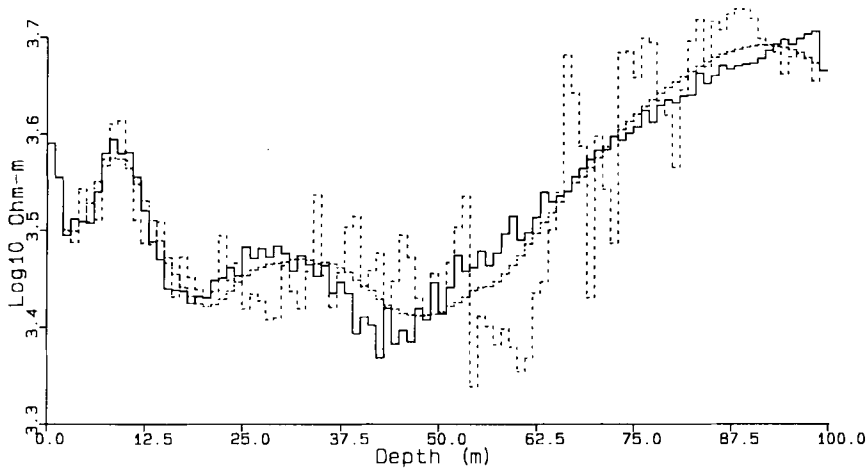

Figure 10. Inversion results for the BH3 simulated sounding: longer dashed line represents the true (logged) resistivities, solid line is f^0 inversion (white noise covairance model), dotted line is f^{-1} inversion (scaling noise covariance model using the approximate inverse proportionality relationship). The starting model for all inversions is a half-space of resistivity 3000 Ω m.

to the layer resistivities with bases at 23 and 61 m depth. The kernels for $\alpha = 0$ and -1.5 are similar, especially in the vicinity of the parameter that the kernels are centred on. The scaling noise model leads to some oscillatory behaviour at shallow depths, a phenomenon noted by Oldenburg (1978) who used Backus–Gilbert theory for resistivity inversion. As expected, the width of the main peak of the kernels increases with layer depth, indicating that only the larger scale features in the solution are to be trusted as the depth of investigation of the sounding is increased. Fig. 8 shows the *a posteriori* parameter correlations for the two selected layers at 23 and 61 m depth. Using $\alpha = 0$ results in virtually uncorrelated layer parameters indicated by the sharply peaked covariance functions. This is unrealistic because the sounding data cannot resolve such small-scale structure at such depths. Using $\alpha = -1.5$, gives correlation lengths of 3 m for the resistivity at 23 and 4 m for the 61 m layer. This increase in width of the zone in which parameters are highly correlated (correlation coefficient >0.5) increases with depth due to the decreased resolving power of the data. Tarantola & Valette (1982) have advocated use of the matrix **C** instead of **R** for solution appraisal, since measures of the parameter resolution can be taken from the correlation lengths between parameters. However, as the above example illustrates, the use of **C** for such a purpose will only be successful to the degree of how realistic the *a priori* information is.

Figure 9 shows the reduction in the standard deviation of the parameters provided by the measurements as a function of the scaling exponent α. For $\alpha = 0$, the improvement is only significant for the first few (shallow) layers and the lower half-space, while the remaining parameters show only a small reduction in variance. In contrast, using the appropriate value of $\alpha = -1.5$, even the poorly determined lower layers generally show a greater than two-fold decrease in parameter standard deviation.

The clustering of values of α around -1 (Table 1) suggests that if the exact value of α is not known, $\alpha = -1$ can be used. As Fig. 10 illustrates, this yields results very similar to those using the exact α. Again, the improvement over the case $\alpha = 0$ is notable.

CONCLUSIONS

It is remarkable that power spectra of a variety of geophysical variables show scaling noise behaviour over at

least some range of spatial frequencies in the logs we have examined. It is even more remarkable that the scaling exponent α determined from the spectra is approximately -1, varying from -1.9 to -0.42 if we exclude the reflection coefficients. The geological origins of this behaviour are unclear. Only study of more logs and the associated geology can tell us to what extent the values we have found are typical of a given geophysical variable in a particular geological setting. We have given reasons for preferring a value of -1. The departure from -1 may be a second-order problem but it is clearly an important one.

The implications of non-zero α are clearly far-reaching and, in any event, the common assumption of whiteness of parameters is inadequate. We have shown that the use of the exact value of α in resistivity sounding inversion leads to reliable statistics for the final parameter estimates and solutions that are structurally simple, containing the minimum amount of complexity demanded by the data. In the case when the exact value of α is unknown, using $\alpha = -1$ yields satisfactory results.

Inversions for other variables in the 1-D case would show similar improvements but the greatest benefit of these observations is likely to lie in higher dimensional inversions. There is good evidence that rock porosity shows scaling behaviour in 3-D on the basis of multiple logs in oil fields (Hewett 1986) and it is likely that other geophysical variables will show the same behaviour, an important key to the 3-D structure of the Earth. Higher dimensional inversions of EM and MT data, for example, suffer from a lack of realistic constraints which must be artificially introduced, such as an arbitrary smoothing of the model. The scaling noise covariance may provide the constriants needed to derive a realsitic model.

ACKNOWLEDGMENTS

We would like to thank an anonymous reviewer from *Geophysical Research Letters* for encouraging us to undertake the inversion problem. We also thank Oliver Jensen for helpful discussions and Gord Bernius for the initial processing of the borehole data. Contribution of the Geological Survey of Canada 11089.

REFERENCES

Angelier, J. A., Tarantola, A., Manoussis, S. & Valette, B., 1982. Inversion of field data in fault tectonics to obtain the regional stress tensor, *Geophys. J. R. astr. Soc.*, **69,** 607–621.

Backus, G., 1970. Inference from inadequate and inaccurate data: II, *Proc. Natl. Acad. Sci.*, **65,** 281–287.

Backus, G., 1988. Bayesian inference in geomagnetism, *Geophys. J. R. astr. Soc.*, **92,** 125–142.

Backus, G. & Gilbert, F., 1970. Uniqueness in the inversion of inaccurate gross earth data, *Phil. Trans. R. Soc. Lond.*, A, **266,** 123–192.

Bernius, G. R., 1981. Boreholes near Ottawa for the development and testing of borehole logging equipment—a preliminary report, in *Current Research, Part C,* Geological Survey of Canada, Paper 81–1C, pp. 51–53.

Bloxham, J., 1987. Simultaneous stochastic inversion for geomagnetic main field and secular variation. 1. A large-scale inverse problem, *J. geophys. Res.*, **92,** 11 597–11 608.

Constable, S. C., Parker, R. L. & Constable, C. G., 1987. Occam's inversion: A practical algorithm for generating smooth models for electromagnetic sounding data, *Geophysics,* **52,** 289–300.

Duijndam, A. J. W., 1988. Bayesian estimation in seismic inversion. Part I: Principles, *Geophys. Prosp.*, **36,** 878–898.

Feder, J., 1988. *Fractals,* Plenum Press, New York.

Franklin, J. N., 1970. Well-posed stochastic extensions of ill-posed linear problems, *J. Math. Analysis Appl.*, **31,** 682–716.

Gubbins, D. & Bloxham, J., 1985. Geomagnetic field analysis—III. Magnetic fields on the core–mantle boundary, *Geophys. J. R. astr. Soc.*, **80,** 695–714.

Hewett, T. A., 1986. Fractal distributions of reservoir heterogeneity and their influence on fluid transport, *61st Annual Technical Conference, Society of Petroleum Engineers,* New Orleans.

Hosken, J. W. J., 1980. A stochastic model of seismic reflections, *50th Annual Meeting, Society of Exploration Geophysicists,* Houston.

Jackson, D. D., 1979. The use of *a priori* data to resolve non-uniqueness in linear inversion, *Geophys. J. R. astr. Soc.*, **57,** 137–158.

Jensen, O. G., Todoeschuck, J. P., Crossley, D. J. & Gregotski, M. E., 1990. Fractal linear models of geophysical processes, in *Non-Linear Variability and Geophysics,* eds Lovejoy, S. & Schertzer, D., Reidel, Dordrecht, in press.

Kanasewich, E. R., 1981. Time sequence analysis in geophysics, University of Alberta Press, Alberta.

Koefed, O., 1979. *Geosounding Principles, 1. Resistivity Sounding Measurements,* Elsevier, Amsterdam.

Mandelbrot, B. B., 1983. *The Fractal Geometry of Nature,* W. H. Freeman, San Francisco.

Marquardt, D. W., 1963. An algorithm for least squares estimation of nonlinear parameters, *Soc. Indust. Appl. Math.*, **11,** 431–441.

Meyerholtz, K. A., Pavlis, G. L. & Szpakowski, S. A., 1989. Convolutional quelling in seismic tomography, *Geophysics,* **54,** 570–580.

Montagner, J.-P. & Jobert, N., 1988. Vectorial tomography—II. Application to the Indian Ocean, *Geophys. J. R. astr. Soc.*, **94,** 309–344.

Nowack, R. L. & Lutter, W. J., 1988. A note on the calculation of covariance and resolution, *Geophys. J. R. astr. Soc.*, **95,** 205–207.

Oldenburg, D. W., 1978. The interpretation of direct current resistivity measurements, *Geophysics,* **43,** 610–625.

Parker, R. L., 1988. A statistical theory of seamount magnetism, *J. geophys. Res.*, **93,** 3105–3115.

Parker, R. L. & Shure, L., 1982. Efficient modelling of the Earth's magnetic field with harmonic splines, *Geophys. Res. Lett.*, **9,** 812–815.

Robinson, E. A., 1957. Predictive decomposition of seismic traces, *Geophysics,* **22,** 767–778.

Spector, A. & Grant, F. S., 1970. Statistical models for interpreting aeromagnetic data, *Geophysics,* **35,** 293–302.

Tarantola, A., 1987. *Inverse Problem Theory. Methods for Data Fitting and Model Parameter Estimation,* Elsevier, Amsterdam.

Tarantola, A. & Valette, B., 1982. Generalized nonlinear inverse problems solved using the least squares criterion, *Rev. Geophys. Space Phys.*, **20,** 291–232.

Tarantola, A. & Nercessian, A., 1984. Three-dimensional inversion without blocks, *Geophys. J. R. astr. Soc.*, **76,** 299–306.

Tikhonov, A. N., 1963. Resolution of ill-posed problems and the regularization method, *Dokl. Akad. Nauk. SSSR,* **151,** 501–504.

Todoeschuck, J. P. & Jensen, O. G., 1988. Joseph geology and seismic deconvolution, *Geophysics,* **53,** 1410–1414.

Todeschuck, J. P. & Jensen, O. G., 1989. Scaling geology and seismic deconvolution, *Pure appl. Geophys.*, **131,** 273–288.

Todeschuck, J. P., Jensen, O. G. & Labonte, S., 1990. Gaussian scaling noise model of seismic reflection sequences: Evidence from well logs, *Geophysics*, in press.

van de Meulebrouck, J., Bayer, R. & Burg, J.-P., 1984. Density and magnetic tomography of the upper continental crust: application to a thrust area of the french Massif Central, *Ann. Geophys.*, **2**, 579–592.

Walden, A. T. & Hosken, J. W. J., 1985. An investigation of the spectral properties of primary reflection coefficients, *Geophys. Prosp.*, **33**, 400–435.

Walden, A. T. & Hosken, J. W. J., 1986. The nature of the non-Gaussianity of primary reflection coefficients and its significance for deconvolution, *Geophys. Prosp.*, **34**, 1038–1066.

Wiggins, R. A., 1972. The general linear inverse problem: implication of surface waves and free oscillations for Earth structure, *Rev. Geophys. Space Phys.*, **10**, 251–285.

Wu, R. S. & Aki, K., 1985. The fractal nature of the inhomogeneities in the lithosphere evidenced from seismic wave scattering, *Pure appl. Geophys.*, **123**, 805–818.